J. Phys. G: Nucl. Part. Phys. 21 (1995) 657–668. Printed in the UK

# Mean-field calculations of proton and neutron distributions in Sr, Xe and Ba isotopes

A Baran†, J L Egido‡, B Nerlo-Pomorska†, K Pomorski†, P Ring§ and L M Robledo‡

† Zakład Fizyki Teoretycznej, Uniwersytet M.C.S., Lublin, Poland

‡ *Departamento de Fisica Teórica, Universidad Autónoma, Madrid, Spain*

§ Technische Universität München, Garching, Germany

Received 10 May 1994, in final form 8 December 1994

**Abstract.** The mean-square nuclear radii, quadrupole moments and deformation parameters of the proton and neutron distributions are evaluated using the mean-field Hamiltonians with the Gogny and Skyrme forces. The results are compared with the estimates obtained within the relativistic mean-field theory and with the experimental data. The calculations were performed for a few sets of the Skyrme forces and for a wide range of the neutron numbers of Sr, Xe and Ba isotopes. A significant difference was found in the deformation of the proton and neutron distributions, especially for Sr isotopes.

## 1. Introduction

The aim of this work is to analyse the application of a few mean-field models to the description of sizes and shapes of neutron and proton distributions in the ground state of nuclei for a wide range of neutron numbers.

Many authors present their models with different parameter sets in order to reproduce several features of nuclei, but it seems that up to now a broad comparison of the theoretical results and the experimental data fails, especially for nuclei far from the $\beta$-stability line. To describe these isotopes properly one has to choose a model sensitive to the subtle effects of the neutron excess in a nucleus which also reproduces the data on the borders of nuclear regions, far from the magic proton ($Z$) and neutron ($N$) numbers.

It seems that for these nuclei qualitatively new events appear with increasing neutron numbers, which can throw new light on the nature of nucleon–nucleon interaction, especially its isospin dependence. In our analysis, the results obtained with the effective Skyrme nucleon–nucleon interaction [1, 2] are compared with those evaluated with the Gogny forces [3, 4] and the relativistic mean-field (RMF) theory [5, 6].

We have calculated the mean-square charge radii (MSR) and electric quadrupole moments ($Q_2$) of Sr, Xe and Ba isotopes. The equilibrium deformations and root-mean-square radii of proton and neutron distributions are also compared. The results with the Gogny forces are similar to those obtained with the RMF theory, while the Skyrme forces Sk1–Sk7 give slightly worse MSR values. Only the estimates obtained in [2] in the semiclassical approach to the HF–BCS method for the set of Skyrme forces SkSC4 are as good as those obtained within RMF and Gogny models. Significant differences in the equilibrium deformations of the proton and neutron distributions for the neutron-rich Sr isotopes are found for the

Skyrme forces and the RMF theory. In addition, the root-mean-square radius of neutrons has been shown to increase more rapidly with the neutron number than that of protons. This increase is especially large for estimates obtained within the RMF theory.

Our theoretical estimates of the quadrupole moments are only static, i.e. no dynamical effects [7] are included here. This is probably the reason why the theoretical values of $Q_2$ for less deformed nuclei are systematically smaller than the experimental data.

## 2. The theoretical model

The Hartree–Fock calculation with effective interactions, i.e. the nucleon–nucleon forces in the presence of other finite-number nucleons, seems to be the best compromise between the phenomenological mean-field models and the real treatment of the nuclear many-body problem which is unsolvable for heavier nuclei.

The best effective interactions currently available are the Gogny [3] and Skyrme [1, 8] forces. These density-dependent interactions have still not been fully explored to describe the nuclear features. They go beyond the known mean-field theories. Only the relativistic mean-field (RMF) theory [5], having the proper spin–orbit term and treating the nucleon and meson interaction on the more microscopic relativistic level, can be compared with these effective forces. In the following, we present a short description of these three models and their parameters.

### *2.1. Gogny forces*

The finite-range Gogny forces permit a simple inclusion of pairing interactions. It has already been proved that these forces can reproduce the main properties of spherical and deformed nuclei.

The two-body effective potential is:

$$\begin{aligned} V_{12} = \sum_{i=1}^{2} \exp\left(-\frac{|\vec{r}_1-\vec{r}_2|}{\mu_i^2}\right)(W_i + B_i P_\sigma - H_i P_\tau - M_i P_\sigma P_\tau) \\ +t_3(1+x_0 P_\sigma)\delta(\vec{r}_1-\vec{r}_2)\left[\rho\left(\frac{\vec{r}_1+\vec{r}_2}{2}\right)\right]^\gamma \\ +\mathrm{i} W_{\mathrm{LS}} \overleftarrow{\nabla}_{12} \wedge \delta(\vec{r}_1-\vec{r}_2)\overrightarrow{\nabla}_{12}\cdot(\vec{\sigma}_1+\vec{\sigma}_2) + V_{\mathrm{Coul}}. \end{aligned} \tag{1}$$

In the calculations we use the DS1 parametrization of the Gogny force. This was first used in [9] and parameters can be found in [10]. The complete set of these parameters, namely $W_i$, $B_i$, $H_i$, $M_i$, $W_{\mathrm{LS}}$, $x_0$ and $\gamma$ is shown in table 1 [9].

We have performed the Hartree–Fock–Bogolubov (HFB) calculation and obtained the ground state wavefunction. The multipole moments are evaluated as the expectation values of the corresponding operators.

**Table 1.** Set of parameters of the Gogny interaction taken from [9], used in (1).

| Central term | $\mu$ (fm) | W | B | H | M |
|---|---|---|---|---|---|
| $i=1$ | 0.7 | −1720.3 | 1300.0 | −1815.5 | 1397.6 |
| $i=2$ | 1.2 | 103.64 | −163.48 | 162.81 | −223.93 |
| Density term | | $t_3 = 1390.6$ MeV fm$^4$ $x_0 = 1$ $\gamma = 1/3$ | | | |
| Spin–orbit term | | $W_{LS} = -130.0$ MeV fm$^5$ | | | |

### 2.2. *Skyrme forces*

The zero-range, density-dependent Skyrme interaction is simpler than the Gogny forces but it also allows the simultaneous reproduction of nuclear radii and binding energies. These forces are only valid for rather low relative momenta. Here, a short-range expansion of the 'true' interaction $V_{12}$ is used, keeping only the first few terms of the Taylor expansion in the momentum space.

The corresponding two-body interaction has the following form:

$$\begin{aligned} V_{12} = {} & t_0(1+x_0P_\sigma)\delta(\vec{r}_1-\vec{r}_2) - \frac{1}{2}t_1(1+x_1P_\sigma)\left[\overleftarrow{\nabla}_{12}^2\delta(\vec{r}_1-\vec{r}_2)+\delta(\vec{r}_1-\vec{r}_2)\overrightarrow{\nabla}_{12}^2\right] \\ & - t_2(1+x_2P_\sigma)\overleftarrow{\nabla}_{12}\delta(\vec{r}_1-\vec{r}_2)\overrightarrow{\nabla}_{12} \\ & + \frac{1}{6}t_3(1+x_3P_\sigma)\left[\rho_{q_1}(\vec{r}_1)+\rho_{q_2}(\vec{r}_2)\right]^\gamma \delta(\vec{r}_1-\vec{r}_2) \\ & - \mathrm{i}W_0\overleftarrow{\nabla}_{12}\wedge\delta(\vec{r}_1-\vec{r}_2)\overrightarrow{\nabla}_{12}\cdot(\vec{\sigma}_1+\vec{\sigma}_2)+V_{\mathrm{Coul}}. \end{aligned} \tag{2}$$

The parameters of the interaction are listed in table 2 for a few commonly used forces.

**Table 2.** Different sets of parameters of the Skyrme forces (2) used in our estimates.

| Parameter | Sk1 | Sk3 | Sk6 | Sk7 | SkSC4 |
|---|---|---|---|---|---|
| $t_0$ (MeV fm$^3$) | −1057.3 | −1128.75 | −1101.81 | −1096.80 | −1789.42 |
| $t_1$ (MeV fm$^5$) | 235.9 | 395.0 | 271.67 | 246.2 | 283.467 |
| $t_2$ (MeV fm$^5$) | −100.0 | −95.0 | −138.33 | −148.0 | −283.467 |
| $t_3$ (MeV fm$^4$) | 14463.5 | 14000.0 | 17000.0 | 17626.0 | 12782.3 |
| $x_0$ | 0.5634 | 0.45 | 0.583 | 0.62 | 0.79 |
| $x_1$ | 0 | 0 | 0 | 0 | −0.5 |
| $x_2$ | 0 | 0 | 0 | 0 | −0.5 |
| $x_3$ | 0 | 1 | 1 | 1 | 1.13871 |
| $W_0$ (MeV fm$^5$) | 120.0 | 120.0 | 115.0 | 112.0 | 124.877 |
| $\gamma$ | 1 | 1 | 1 | 1 | 0.3333333 |

Using the Hartree–Fock mean-field approximation one can express the total energy of a nucleus as the volume integral:

$$E = \int H(\vec{r})\,\mathrm{d}^3\vec{r}. \tag{3}$$

The energy density $H(\vec{r})$ is a function of nucleon ($\rho$), kinetic energy ($\tau$) and spin ($\vec{J}$) densities. The total energy (3) has to be minimized with respect to the choice of the many-body wavefunctions, which leads to the eigenproblem with the corresponding mean-field Hamiltonian. Unfortunately, the Skyrme forces fail when one tries to obtain the pairing correlations. The residual pairing forces have to be artificially added to the mean-field Hamiltonian in a similar way to in the calculations with the average single-particle Hamiltonians, i.e. we work with the typical BCS formalism. We took the experimental pairing gaps $\Delta$ as calculated from the mass tables of Audi and Wapstra [11] and Möller *et al* [12] for experimentally unknown nuclei. This means that we have solved the equation only for particle numbers in order to determine the position of the Fermi level. We have taken 10 oscillator shells when performing the calculation for Sr isotopes and 12 shells for Xe and Ba isotopes.

*2.3. Relativistic mean-field theory*

The RMF theory starts from a Lagrangian containing nucleonic and mesonic degrees of freedom [5]. In comparison with the density-dependent Hartree–Fock calculations with the Skyrme and Gogny forces, the RMF theory seems to be more fundamental, giving a relativistic treatment of nucleonic and mesonic variables and a proper description of the spin–orbit interactions. Nevertheless, it is still an effective phenomenological method based on the local densities and fields, while numerically it is not much more complicated than the calculation with the Skyrme forces.

The RMF theory was successfully used to reproduce parameters of the nuclear matter and some properties of finite nuclei such as binding energies, mean-square charge radii and quadrupole moments.

The theory is based on the following field Lagrangian density [5, 6]

$$
\begin{aligned}
\mathcal{L} = \bar{\psi}_i\{i\gamma^\mu\partial_\mu - M\}\psi_i &+ \frac{1}{2}\partial^\mu\sigma\partial_\mu\sigma - U(\sigma) - g_\sigma\bar{\psi}_i\psi_i\sigma \\
&-\frac{1}{4}\Omega^{\mu\nu}\Omega_{\mu\nu} + \frac{1}{2}m_\omega^2\omega^\mu\omega_\mu - g_\omega\bar{\psi}_i\gamma^\mu\psi_i\omega_\mu \\
&-\frac{1}{4}\vec{R}^{\mu\nu}\vec{R}_{\mu\nu} + \frac{1}{2}m_\rho^2\vec{\rho}^\mu\vec{\rho}_\mu - g_\rho\bar{\psi}_i\gamma^\mu\vec{\tau}\psi_i\vec{\rho}_\mu \\
&-\frac{1}{4}F^{\mu\nu}F_{\mu\nu} - e\bar{\psi}_i\gamma^\mu\frac{(1-\tau_3)}{2}\psi_i A_\mu\,.
\end{aligned}
\tag{4}
$$

The fields belong to nucleons (Dirac spinor field $\psi$), the low-mass isovector–vector meson ($\vec{\rho}_\mu$; $\vec{R}_{\mu\nu}$), the isoscalar–vector ($\omega_\mu$; $\Omega_{\mu\nu}$), the scalar $\sigma$ and the massless photon vector field ($A_\mu$; $F_{\mu\nu}$). The field tensors are given by

$$\Omega^{\mu\nu} = \partial^\mu\omega^\nu - \partial^\nu\omega^\mu \tag{5}$$

$$\vec{R}^{\mu\nu} = \partial^\mu\vec{\rho}^\nu - \partial^\nu\vec{\rho}^\mu - g_\rho(\vec{\rho}^\mu \wedge \vec{\rho}^\nu) \tag{6}$$

$$F^{\mu\nu} = \partial^\mu A^\nu - \partial^\nu A^\mu. \tag{7}$$

In (4), the $U(\sigma)$ potential represents fields in which $\sigma$-mesons are moving. It has the form

$$U(\sigma) = \frac{1}{2}m_\sigma\sigma^2 + \frac{1}{3}g_3\sigma^3 + \frac{1}{4}g_4\sigma^4. \tag{8}$$

The case $g_3 = g_4 = 0$ corresponds to a linear Walecka model [5]

The Dirac spinors $\psi_i$ of the nucleon and the fields of $\sigma$-, $\rho$- and $\omega$-mesons are solutions of the coupled Dirac and Klein–Gordon equations which are obtained from (4) by means of the classical variational principle and are then solved (in the static case) by the self-consistent Hartree method for the case of axially-symmetric systems of nucleons with additional pairing interaction. These equations are solved iteratively; starting from an estimate of the meson and electromagnetic fields, one can solve the Dirac equation and obtain the spinors $\psi_i$. These are used to obtain the densities and currents. The latter serve as sources for solution of the Klein–Gordon equations and provide the new estimates of the meson and electromagnetic fields for the next iteration [6].

The parameters used in our calculation are [6]:

- $M$, the nucleon mass,
- $m_\sigma, m_\omega, m_\rho$, the meson masses,
- $g_\sigma, g_\omega, g_\rho$, the meson coupling constants,
- $e^2/4\pi = 1/137$, the photon coupling constant, and
- $g_3, g_4$, the $\sigma$-meson field constants.

All the nucleon coupling constants $g_\omega$, $g_\rho$, $g_\sigma$, the mass of the $\sigma$-field, and $g_3$ and $g_4$ are listed in table 3 and are taken from [13].

**Table 3.** The parameters set NL–SH [13] used in the relativistic mean-field Lagrangian, (4).

| Parameter | Value |
|---|---|
| $M$ (MeV) | 939.0 |
| $m_\sigma$ (MeV) | 526.059 |
| $m_\omega$ (MeV) | 783.00 |
| $m_\rho$ (MeV) | 763.00 |
| $g_\sigma$ | 10.4444 |
| $g_\omega$ | 12.945 |
| $g_\rho$ | 4.383 |
| $g_2$ | −6.9099 |
| $g_3$ | −15.8337 |

Similarly to in the mean-field calculations with the Skyrme forces, we added external monopole-pairing correlations with the strength which would reproduce exactly the experimental pairing energy gaps for each isotope considered. In addition, we have taken the basis consisting of 10 oscillator shells for Sr and 12 shells for Xe and Ba isotopes.

### *2.4. Mean-field estimates of nuclear size and shape*

We are interested in the quantities characterizing the neutron and proton distribution in nuclei, their sizes and shapes. In order to obtain estimates of these quantities for nuclei far from $\beta$-stability we have applied all three mean-field methods described above.

The mean-square radius (MSR) of the neutron (or proton) distribution is equal to the expectation value of the operator $\vec{r}^{\,2}$ between the corresponding Hartree–Fock–Bogolubov wavefunctions $|HFB>$ :

$$\langle \vec{r}^{\,2}\rangle_{n,p} = \langle \mathrm{HFB}(n,p)|\vec{r}^{\,2}|\mathrm{HFB}(n,p)\rangle. \tag{9}$$

The experimental data supplied us with the charge radius rather than the proton radius [14, 15]. The theoretical charge radius is equal to that of protons corrected on the finite proton charge distribution

$$\langle \vec{r}^{\,2}\rangle_{\mathrm{ch}} = \langle \vec{r}^{\,2}\rangle_{p} + 0.64\ \mathrm{fm}^2. \tag{10}$$

We have neglected here the contributions to the charge mean-square radius originating from the electron-neutron form factor and the electromagnetic spin–orbit coupling [16, 17]. For the nuclei Sr to Ba considered in our paper the two corrections are of the same order (approximately 0.1 $\mathrm{fm}^2$) but have different signs; thus, their effect on $\langle \vec{r}^{\,2}\rangle_{\mathrm{ch}}$ is much smaller than the typical differences between the results obtained by us within various theoretical models.

The global measure of the deformation of the neutron (or proton) distribution could be expressed by the corresponding quadrupole moment

$$\langle Q_2\rangle_{n,p} = \langle \mathrm{HFB}(n,p)|2r^2P_2(cos(\theta)|\mathrm{HFB}(n,p)\rangle. \tag{11}$$

Having the quadrupole and monopole moments we can estimate approximately the deformation parameter $\beta$ of the neutron (or proton) distribution [18]

$$\beta_{n,p} = \sqrt{\frac{4\pi}{5}}\frac{\langle Q_2\rangle_{n,p}}{\langle Q_0\rangle_{n,p}} \tag{12}$$

where $\langle Q_0\rangle_n = N\langle\vec{r}^2\rangle_n$ and $\langle Q_0\rangle_p = Z\langle\vec{r}^2\rangle_p$. This simple estimate for the quadrupole deformation is only valid for small deformations $\beta$.

## 3. Results

The calculations were performed for Sr, Xe and Ba isotopes for which the experimental data of MSR [14] and their isotopic shifts [15] is available. All these elements have a large number of isotopes and show an interesting 'kink' effect, i.e. the rapid growth of nuclear radius when reaching the magic number 50 for Sr or 82 for Xe and Ba. Unfortunately, this effect is not reproduced in most of the theoretical calculations.

In figures 1–3 the charge MSR values of Sr (figure 1), Xe (figure 2) and Ba (figure 3) are drawn as a function of the neutron number $N$. In figure 1($a$) the results obtained with the Gogny forces (solid line) and those for the RMF method (dashed line) are compared with the experimental data (crosses) taken from [14, 15]. Similar results obtained with the Skyrme forces Sk1 (solid line), SkSC4 (dashed line) and Sk7 (short dashes) are plotted in figure 1($b$). The theoretical values of $r^2$ and $Q_{20}$ for the SkSC4 forces are taken from [2] and were obtained within the semiclassical approximation. The charge MSR values obtained for Xe isotopes are plotted in figures 2($a$), ($b$) and those for Ba in figures 3($a$), ($b$).

In general, the RMF theory, the Gogny forces and the set SkSC4 of the Skyrme forces give the best MSR estimates. The Skyrme calculation with the set of parameters Sk7 gives larger MSR values for every element, while the set Sk1 gives values that are too small. We have also performed the calculations using the Sk3 and Sk6 forces, but the results obtained with these were always close to those for Sk7 and therefore we have not presented them in our figures.

One can see that for Sr isotopes the Gogny forces give slightly too large values of MSR and that they are unable to reproduce the change in the systematics of MSR when passing the magic number $N = 50$. Neither do the theoretical estimates of RMF theory reproduce this 'kink' properly, although one has to say that the RMF values of MSR for Sr are closer to the experimental points than those of Gogny. More extended discussion of the results of the RMF model for Sr isotopes can be found in [19]. A discussion of the ground-state properties of Sr isotopes together with experimental data for radii and quadrupole moments are also given in [20] where forces SKa and G0P were used.

The values obtained with the Sk7 forces are too large, while, surprisingly, the Sk1 set gives the closest estimates of the MSR values to the experimental data for all Sr isotopes.

It is interesting that for the Xe and Ba elements neither the Sk7 nor the Sk1 set gives a good estimate of the charge radii. The MSR values with Sk1 are too small, while those for Sk7 to large. The values obtained with the Gogny forces or the Skyrme interaction SkSC4 and the RMF theory for all Xe and Ba isotopes are very close to the experimental data.

In all three models, the theoretical estimates of MSR for neutrons increase with the neutron number. For heavier isotopes these MSR values are larger than those for protons. This so-called 'neutron-skin' effect was observed experimentally for heavier isotopes (see e.g. [21]). Here we would like to show how the size of the neutron skin depends on the model and the parameters of the forces.

In figures 4–6 the difference between the theoretical values of the root-mean-square radius of neutrons ($R_n$) and protons ($R_p$) is plotted as the function of mass number for Sr, Xe and Ba elements. The results obtained with the Gogny forces are represented by the solid line, the data obtained within the RMF theory by the dashed line and those for the Sk7 Skyrme interaction by the short dashes. One can see that in all three theoretical models the width of the neutron skin grows with the neutron number. The estimates obtained within

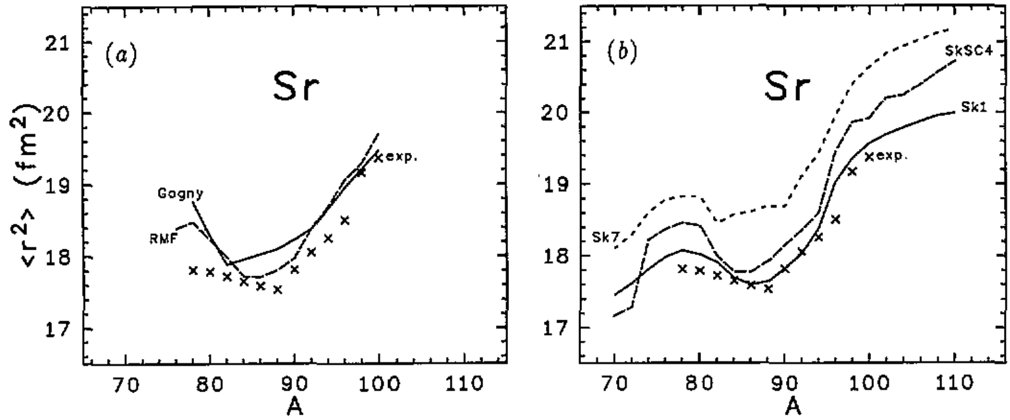


**Figure 1.** The theoretical estimates of the root mean square radius for Sr isotopes. The results obtained with the Gogny forces (solid line) and in the RMF theory (dashed line) are compared in (*a*) with the experimental data (crosses) taken from [16, 17]. The estimates obtained with the Skyrme forces for the Sk1 (solid line), SkSC4 (dashed line) and Sk7 (short dashes) are plotted in (*b*).

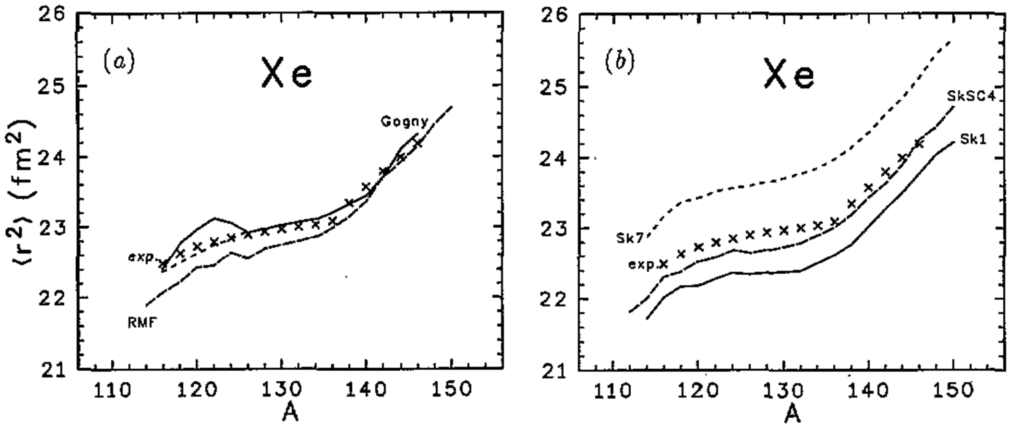


**Figure 2.** The same as in figure 1(*a*), (*b*) but for Xe isotopes.

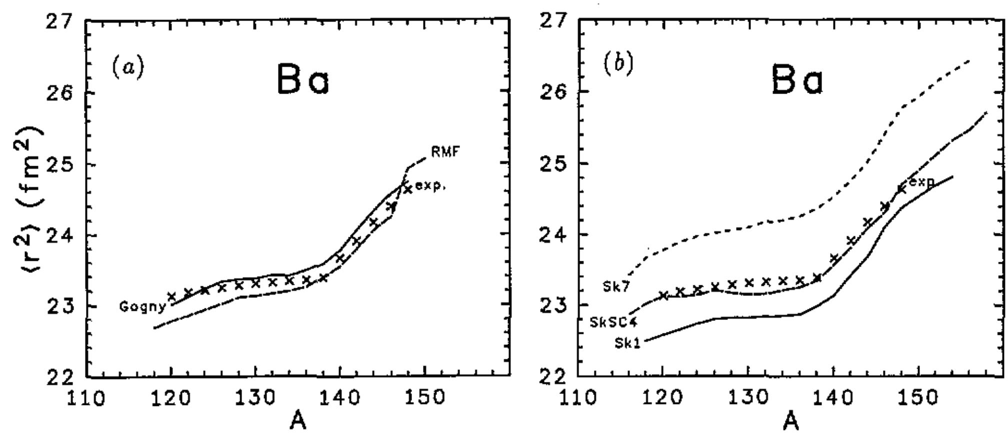


**Figure 3.** The same as in figure 1(*a*), (*b*) but for Ba isotopes.

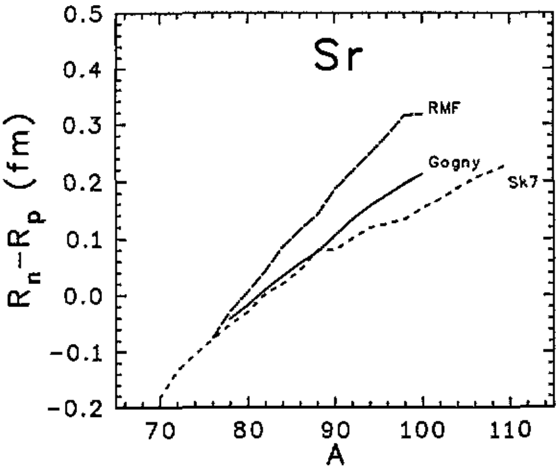


**Figure 4.** The theoretical estimates of the difference between the neutron and proton mean-square radii for Sr isotopes. The results obtained with Gogny forces (solid line) are compared with those obtained within the RMF theory (dashed line) and with the Sk7 Skyrme interaction (short dashes).

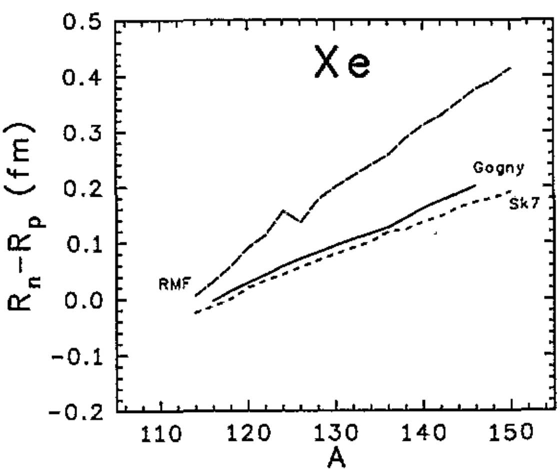


**Figure 5.** The same as in figure 4 but for Xe isotopes.

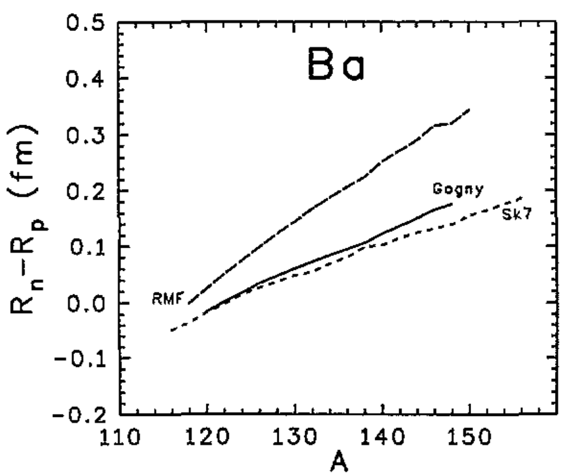


**Figure 6.** The same as in figure 4 but for Ba isotopes.

the Gogny and Skyrme model are similar, while the RMF theory predicts a larger growth. The neutron-skin width reaches the value 0.4 fm for the heavier isotopes.

We have also studied the difference between deformations of proton and neutron distributions. Using (12) we have estimated the quadrupole deformation of both distributions. A typical difference between the absolute value of the proton and neutron deformations is $\Delta\beta \approx 0.01$. Only for Sr isotopes and the estimates obtained with the RMF model have we noticed a more significant difference in deformations of proton and neutron distributions. These results are plotted in figures 7–9 for Sr, Xe and Ba isotopes respectively. It can be seen that for the neutron-rich isotopes the proton distributions are systematically more deformed than the neutron ones. The maximum difference $\Delta\beta$ of order 0.04 was found in RMF for heavier Sr isotopes. The ground-state deformation of these isotopes is around $\beta = 0.3$.

The theoretical estimates of the electric quadrupole moment for Sr, Xe and Ba isotopes are presented in figures 10–12. The results are obtained using the three methods described above. It can be seen that the theoretical estimates for less deformed nuclei are systematically smaller than the experimental data. This is probably due to the lack of the dynamical effects in our analysis [7].

In addition, for $^{78-80}$Sr isotopes we have found non-axial ground-state deformations ($\gamma \sim 20^o$) in the estimates made with the Gogny forces. In the other two methods (RMF and Skyrme) the $\gamma$ degree of freedom was not taken into account.

## 4. Conclusions

The following conclusions can be drawn from our investigations:

(i) The Gogny and RMF theories as well as the newest set (SkSC4) of Skyrme forces reproduce the charge mean-square values of Sr, Xe and Ba isotopes very well. The old sets of parameters for the Skyrme interaction give results larger (Sk7) or smaller (Sk1) than the experimental data. For Sr isotopes only the SkI forces give the best estimates of the charge MSR.

(ii) The difference between the root-mean-square radius of neutrons and protons grows almost linearly with the neutron number. This difference also depends significantly on the theoretical model used. The relativistic mean-field theory with NL–SH parameters (table 3) predicts the largest growth.

(iii) The deformations of the proton and neutron distributions are not always close to each other. In heavy Sr isotopes, in Skyrme HFB calculations and in estimates obtained within the RMF theory, significant differences ($\Delta\beta \sim 0.04$) were found.

(iv) The electric quadrupole moments for well-deformed isotopes are reproduced equally well in all three models, while for the less deformed nuclei the static HFB theoretical predictions are always too small.

## Acknowledgments

Krzysztof Pomorski gratefully acknowledges the warm hospitality extended to him by the theoretical physics group of the Universidad Autónoma in Madrid as well as the grant from the Spanish Ministerio de Asuntos Exteriores. Peter Ring would also like to express his appreciation for hospitality shown to him in Lublin and for the financial support from the European Union. The research of J L Egido and L M Robledo is supported by DGICyT,

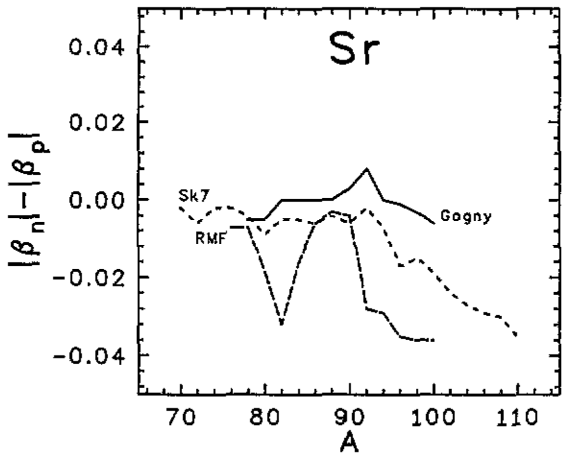


**Figure 7.** The difference between the absolute values of the neutron and proton quadrupole deformations for Sr isotopes. The results obtained with Gogny forces (solid line) are compared with those obtained within the RMF theory (dashed line) and with the Sk7 Skyrme interaction (short dashes).

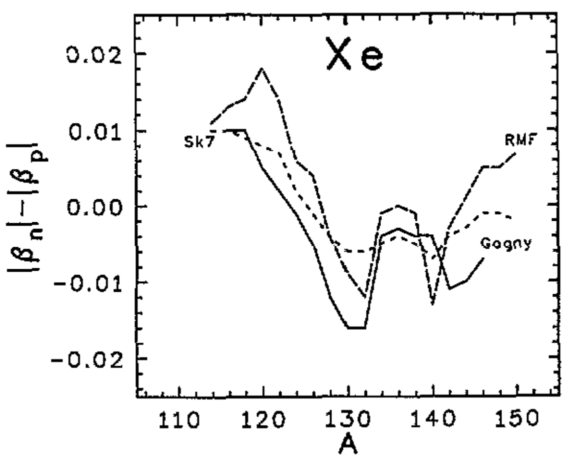


**Figure 8.** The same as in figure 7 but for Xe isotopes.

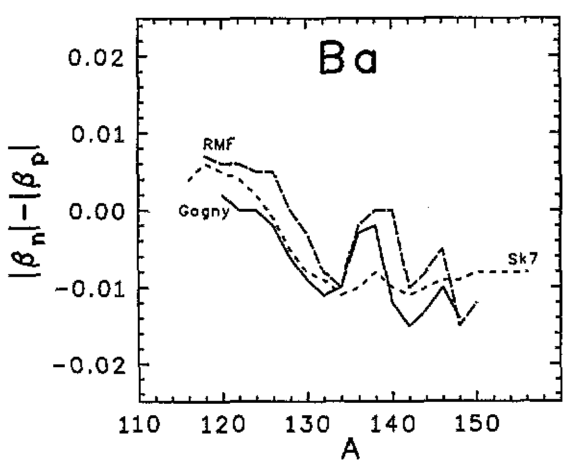


**Figure 9.** The same as in figure 7 but for Ba isotopes.

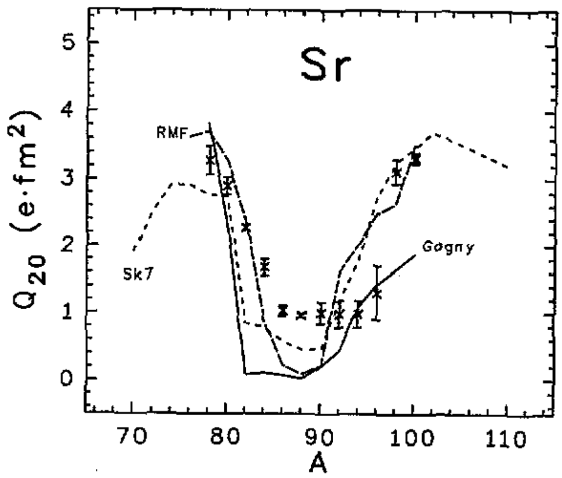


**Figure 10.** The electric quadrupole moments of the Sr isotopes. The results obtained with Gogny forces (solid line), within the RMF theory (dashed line) and with the Sk7 Skyrme interaction (short dashes) are compared with the experimental data (crosses) taken from [22–24].

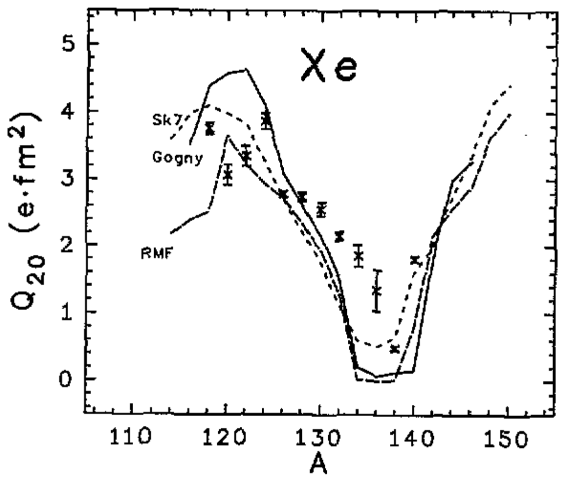


**Figure 11.** The same as in figure 10 but for Xe isotopes. Experimental data (crosses) are taken from [23, 24].

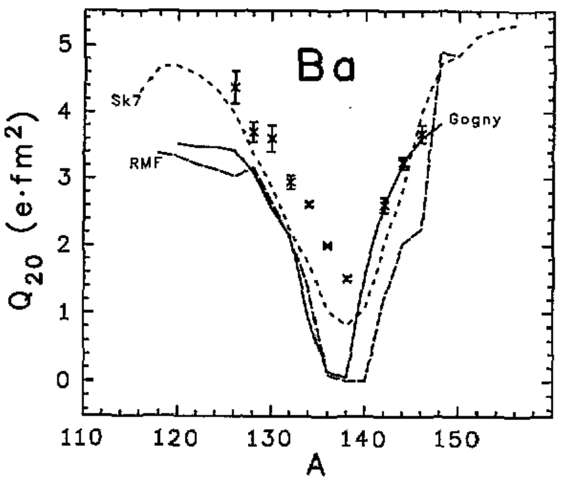


**Figure 12.** The same as in figure 10 but for Ba isotopes. Experimental data (crosses) are taken from [23, 24].

Spain, under project PB91-0006. This work is partly supported by the Polish Committee of Scientific Research under contract no. 2P30205206.

## References

[1] Skyrme I H R 1956 *Phil. Mag.* **1** 1043; 1958 *Nucl. Phys.* **9** 615
[2] Aboussir Y, Pearson J M, Dutta A K and Tondeur F 1992 *Nucl. Phys.* A **549** 155
[3] Gogny D 1975 *Nuclear Self Consistent Fields* ed G Ripka and M Porneuf (Amsterdam: North Holland)
[4] Egido J L and Robledo L M 1989 *Nucl. Phys.* A **494** 85
[5] Serot B D and Walecka J D 1986 The relativistic nuclear many-body problem *Advances in Nuclear Physics* ed J W Negele and E Vogt (New York: Plenum) vol 16
[6] Gambir Y K, Ring P and Thimet T 1990 *Ann. Phys., NY* **198** 132
[7] Nerlo-Pomorska B, Pomorski K and Skorupska-Mach B 1993 *Nucl. Phys.* A **562** 80
[8] Vautherin D and Brink D M 1972 *Phys. Rev.* C **5** 626
Flocard H, Quentin P, Kerman A K and Vauthrin D 1973 *Nucl. Phys.* **203** 3
[9] Berger J F, Girod M and Gogny D 1984 *Nucl. Phys.* A **428** 23c
[10] Robledo L M, Egido J L, Berger J F and Girod M 1987 *Phys. Lett.* **187B** 223
[11] Audi G and Wapstra A H 1993 *Nucl. Phys.* A **565** 1
[12] Möller P, Nix J R, Myers W D and Swiatecki W J 1994 *Preprint* LBL *Atom. Data Nucl. Data Tabl.* in press
[13] Sharma M M, Nagarajan M A and Ring P 1993 *Phys. Lett.* **312** 377
[14] de Vries H, de Jager C W and de Vries C 1987 *Atom. Data Nucl. Data Tabl.* **36** 495
[15] Otten E W 1989 *Treatise on Heavy-Ion Science* ed D A Bromley (New York: Plenum) vol 8
[16] Bertozzi W, Friar J, Heisenberg J and Negele J W 1972 *Phys. Lett.* **41B** 408
[17] Nishimura M and Sprung D W L 1987 *Prog. Theor. Part. Phys.* **77** 781
[18] Hasse R W and Myers W D 1988 *Geometrical Relationships of Macroscopic Nuclear Physics* (Berlin: Springer)
[19] Hirata D, Toki H, Tanihata I and Ring P 1993 *Phys. Lett.* **314B** 168
[20] Buchinger F, Ramsay E B, Arnold E, Neu W, Neugart R, Wendt K, Silverans R E, Lievens P, Vermeeren L, Berdichevsky D, Fleming R, Sprung D W L and Ulm G 1990 *Phys. Rev.* C **41** 2883
[21] Jastrzębski J, Daniel H, v Egidy T, Grabowska A, Kim Y S, Kurcewicz W, Lubiński P, Riepe G, Schmid W, Stolarz A and Wycech S 1992 *Proc. 2nd Biennial Conf. on Low Energy Antiproton Physics (LEAP 92) (Aosta Valley, Italy, September 1992)*; *Nucl. Phys.* A **558** 405c–414c
[22] Mach H, Wohn F K, Molnar G, Sistemich K , Hill J C, Moszynski M, Gill R L, Krips W and Brenner D S 1991 *Nucl. Phys.* A **523** 197–227
[23] Raman S, Malarkey C H, Milner W T, Nestor C W Jr and Stelson P H 1987 *Atom. Data Nucl. Data Tabl.* **36** 1–96
[24] Raman S, Nestor C W Jr, Kahane S and Bhat K H 1989 *Atom. Data Nucl. Data Tabl.* **42** 1–54